Shear Relaxation of Imidazolium-Based Room-Temperature Ionic Liquids

Tsuyoshi Yamaguchi,*,† Sho Miyake,†,‡ and Shinobu Koda†

Department of Molecular Design and Engineering, Graduate School of Engineering, Nagoya University, Furo-cho B2-3(611), Chikusa, Nagoya, Aichi 464-8603, Japan, and Chemical Engineering Course, School of Engineering, Nagoya University, Furo-cho B2-3(611), Chikusa, Nagoya, Aichi 464-8603, Japan

Received: March 17, 2010; Revised Manuscript Received: May 18, 2010

The frequency-dependent shear viscosities of four representative imidazolium-based room-temperature ionic liquids, 1-butyl-3-methylimidazolium bis(trifluoromethanesulfonyl)amide ([bmim][TFSA]), 1-butyl-3-methylimidazolium hexafluorophosphate ([bmim][PF_6]), 1-hexyl-3-methylimidazolium hexafluorophosphate ([hmim][PF_6]), and 1-methyl-3-octylimidazolium hexafluorophosphate ([omim][PF_6]), are measured from 5 to 205 MHz with shear impedance spectroscopy. A relaxation is observed in the measured frequency range in all cases. This is the first report on the shear relaxation of ionic liquids at room temperature, to our best knowledge. Comparing the spectra of the common cations, [bmim][TFSA] and [bmim][PF_6], the normalized relaxation spectra, $\eta(\nu)/\eta_0$, reduce to a single curve when plotted against $\eta_0\nu$, where ν and η_0 stand for the frequency and shear viscosity, respectively. The lower viscosity of the TFSA salt is thus elucidated by the shorter relaxation time. The lower viscosity at higher temperature is also attributed to the shorter relaxation time. On the other hand, the increase in the length of the alkyl chain of the cation leads to the lower-frequency shift of the relaxation frequency on the $\eta_0\nu$ scale. Therefore, the higher viscosity of the omim salt is the result of the compensation of the longer relaxation time for the smaller high-frequency shear modulus. In addition, the relaxation time distribution becomes broader with increasing chain length, which can be ascribed to the heterogeneity of the liquid structure.

1. Introduction

The room-temperature ionic liquid, which is often called simply an ionic liquid, is a molten salt whose melting temperature is below or around room temperature. It is usually composed of organic ions, and we can design properties of ionic liquids by changing the combination of ions.[1,2]

Shear viscosity is one of the important properties of an ionic liquid partly because it can be related to the molecular mobility in liquids. The decrease in the shear viscosity is often required for practical uses, and many ionic liquids of low viscosity have been developed so far. However, it is not clear at present how the molecular structure and interaction of ions affect the shear viscosity.

The shear viscosity is defined as the proportionality coefficient between the shear rate and the shear stress. When the instantaneous shear flow is applied to the liquid, the microscopic structure of the liquid is distorted, which leads to the shear stress. The distorted structure relaxes to the equilibrium state as time goes, and the shear stress decays gradually. When the applied shear flow is sufficiently small, the distortion of the liquid structure is proportional to the shear flow, and the resultant shear stress is described as the superposition of the linear response function. Since the response to the steady shear flow is equal to the time integration of the instantaneous one, the shear viscosity is approximately given by the product of two factors, that is, the amplitude and relaxation time of the response function. The former is the shear modulus against the high-frequency shear distortion, and it represents the rigidity of the liquid structure associated with the shear viscosity. The separation of the effects of these two factors will help us understand the origin of liquid structure associated with the shear viscosity.

The time profile of the response function of the shear stress is accessible experimentally by applying the alternating shear flow with various frequencies. The shear viscosity is independent of frequency when the response of the shear stress is instantaneous. On the other hand, the relaxation, that is, the frequency dependence, appears at the frequency near the reciprocal relaxation time when the response is retarded.

The measurement of the shear relaxation has usually been performed at the frequency below the kHz region in mechanical ways. In the case of ionic liquids, Šantić and co-workers reported that 1-butyl-3-methylimidazolium tetrafluoroborate ([bmim][BF_4]) possesses a shear relaxation in the kHz region at about 200 K.[3] They also measured the frequency dispersion of the ionic conductivity of the same sample in the same frequency region, and these two relaxation spectra are compared in order to discuss the microscopic mechanism of the ionic transport in the ionic liquid. However, their experiments were limited to temperatures far below the ambient one, and we have to perform measurements in the MHz region in order to observe the shear relaxation of ionic liquids at room temperature.

Ultrasonic relaxation is closely related to the shear relaxation in that it depends on both bulk and shear viscosities. The ultrasonic relaxation of several ionic liquids at room temperature was recently reported by two groups. Fukuda and co-workers measured the sound velocity of some ionic liquids in the MHz−GHz regions and found an increase in the sound velocity with frequency.[4] Makino and co-workers reported the sound absorption coefficients of some ionic liquids at three different frequencies between 10 and 100 MHz.[5] On the basis of the amplitude of the ultrasonic relaxation and the zero-frequency

* To whom correspondence should be addressed. E-mail: tyama@nuce.nagoya-u.ac.jp.

† Department of Molecular Design and Engineering, Graduate School of Engineering, Nagoya University.

‡ Chemical Engineering Course, School of Engineering, Nagoya University.

10.1021/jp1024137
Published on Web 06/03/2010

shear viscosity, they argued that there must be shear relaxation in the frequency range that they studied. However, it is generally difficult to separate the contributions of bulk and shear viscosities to the ultrasonic relaxation; therefore, the ultrasonic relaxation is not a suitable way to investigate the microscopic origin of shear viscosity.

Shear impedance spectroscopy is an experimental method to determine the shear viscosity of liquids in the MHz region, which is based on a quartz crystal microbalance with dissipation (QCM-D) technology.[6] It has been applied to shear relaxation of various liquids by Kaatze and co-workers,[7,8] and we recently measured the shear relaxation of lithium ion electrolytes with the same method.[9] In addition to the relaxation measurement, the shear impedance method attracts researchers as a viscometer with small sample volume, and the measurement of ionic liquids was reported recently at a single frequency.[10] In this work, we measure the shear relaxation of some representative imidazolium-based ionic liquids at 5−205 MHz. The cations and anions are varied independently, and their effects on the shear viscosity are discussed in terms of their shear relaxation spectra.

2. Theory

According to the Kubo−Green formula, the shear viscosity of liquid is described by the integration of the time correlation function of shear stress as[11]

$$\eta_0 = \frac{V}{k_B T}\int_0^\infty \langle \sigma_{xz}(0)\sigma_{xz}(t)\rangle \, dt \equiv \int_0^\infty \phi(t)\, dt \qquad (1)$$

where η_0, V, k_B, and T are the zero-frequency shear viscosity, the volume of the system, the Boltzmann constant, and the absolute temperature, respectively, and the off-diagonal part of the time-dependent shear stress tensor is denoted as $\sigma_{xz}(t)$. When the correlation function $\phi(t)$ decays in an exponential way as

$$\phi_D(t) = G_\infty e^{-t/\tau} \qquad (2)$$

the shear viscosity is given by the product of the shear modulus (G_∞) and the relaxation time (τ). More generally, suppose that $\phi(t)$ possesses a universal functional form irrespective of the molecular species and thermodynamic conditions, solely parametrized by its amplitude A and the relaxation time τ as

$$\phi(t) = A\phi_0\left(\frac{t}{\tau}\right) \qquad (3)$$

In such a case, the change in the value of η_0 can be related to the product of A and τ as

$$\eta_0 = A\tau\int_0^\infty \phi_0(t')\, dt' \equiv A\tau\tilde{\phi}_0(0) \qquad (4)$$

The Kubo−Green formula, eq 1, can be extended to describe the frequency-dependent shear viscosity, $\eta(\nu)$, in terms of the correlation function, $\phi(t)$, as

$$\eta(\nu) \equiv \eta'(\nu) - i\eta''(\nu) = \int_0^\infty e^{-2\pi i\nu t}\phi(t)\, dt \qquad (5)$$

where $\eta'(\nu)$ and $\eta''(\nu)$ denote the real and imaginary parts of the shear relaxation spectrum, respectively. By substituting eq 2 into eq 5, we can easily show that the well-known Debye relaxation is obtained when the correlation function decays exponentially as follows

$$\eta_D(\nu) = \frac{\eta_0}{1 + 2\pi i\nu\tau} \qquad (6)$$

When the correlation function behaves as eq 3, the shear relaxation spectrum is given by

$$\frac{\eta(\nu)}{\eta_0} = \frac{\tilde{\phi}_0(\nu\tau)}{\tilde{\phi}_0(0)} = \frac{1}{\tilde{\phi}_0(0)}\tilde{\phi}_0\left(\frac{\eta_0\nu}{A\tilde{\phi}_0(0)}\right) \qquad (7)$$

$$\tilde{\phi}_0(\nu) \equiv \int_0^\infty e^{-2\pi i\nu t}\phi_0(t)\, dt \qquad (8)$$

According to eq 7, the normalized shear relaxation spectra, $\eta(\nu)/\eta_0$, are kept unchanged when the relaxation time is constant. On the other hand, when the relaxation amplitude, A, is constant, the spectra reduce to a single master curve if they are plotted against $\eta_0\nu$. Therefore, comparison of shear relaxation spectra on various axes helps us to understand the origin of the change in the zero-frequency shear viscosity in response to the change in molecular species or thermodynamic conditions.

3. Experiment

3.1. Samples. The ionic liquids used in this work are 1-butyl-3-methylimidazolium bis(trifluoromethanesulfonyl)amide ([bmim][TFSA], η_0 = 50 mPa s at 25 °C),[12] 1-butyl-3-methylimidazolium hexafluorophosphate ([bmim][PF_6], η_0 = 273 mPa s at 25 °C and 120 mPa s at 40 °C),[13] 1-hexyl-3-methylimidazolium hexafluorophosphate ([hmim][PF_6], η_0 = 497 mPa s at 25 °C),[14] and 1-methyl-3-octylimidazolium hexafluorophosphate ([omim][PF_6], η_0 = 734 mPa s at 25 °C and 277 mPa s at 40 °C).[15] All of the samples (>98.0%) were purchased from Tokyo Kasei and dried overnight under vacuum at 60 °C before use.

3.2. Shear Impedance Spectrometer. In shear impedance spectroscopy, the changes in the resonance frequency and bandwidth of an AT-cut quartz crystal before and after the contact with liquid samples are measured to determine the shear viscosity of the sample at the resonance frequency of the crystal, as is the case of QCM-D technology.

The structure of the sample cell to hold the quartz crystal and liquid sample is described elsewhere.[9] The fundamental resonance frequency and the diameter of the quartz crystal are 5 MHz and 14 mm, respectively. The temperature of the sample is controlled within ±0.1 K by flowing thermostatted water through the body of the sample cell. The measurements of all of the samples are performed at 25 °C. In addition, the relaxation spectra of [bmim][PF_6] and [omim][PF_6] are measured at 40 °C.

We employ two electric circuits in order to read the resonance signal of the quartz crystal. The first one is the circuit based on the RF bridge method, which is described in detail elsewhere[9] and used in this work at the frequencies from 5 to 105 MHz. The second one is the reflection method with a vector network analyzer (VNA: Hewlett-Packard, HP8720D). The signal line from the quartz crystal is directly connected to a port of the vector network analyzer, and the complex reflection coefficient, S_{11}, is determined as the function of frequency.

3.3. Data Analysis. The complex transmission and reflection spectra of the circuit without sample liquids in the RF bridge and VNA measurements, respectively, are expressed as

$$V_n(\nu) = a\nu + b + \sum_k \frac{V_{n,k}}{1 + \dfrac{\nu - \nu_{n,k}}{\Delta\upsilon_n}\mathrm{i}} \tag{9}$$

Here, n and k are indices for the order of resonance and spurious modes, respectively. The baselines are approximated as a linear function of the frequency, which is characterized by two complex parameters a and b. The resonance peaks are described by the Lorentz functions, whose peak height, central frequency, and bandwidth are denoted as $V_{n,k}$, $\nu_{n,k}$, and $\Delta\nu_n$, respectively. The band widths of all of the spurious modes are assumed to be the same for simplicity. Since the spectrum analyzer used in the RF bridge method measures solely the amplitude of the transmitted signal, the transmission spectra determined in this method, denoted as $V_{n,\mathrm{RF}}(\nu)$, are given by

$$V_{n,\mathrm{RF}}(\nu) = |V_n(\nu)| \tag{10}$$

On the other hand, the complex reflection coefficients, $S_{n,11}(\nu)$, in the VNA measurements are equal to $V_n(\nu)$ in eq 1 because both phase and amplitude are determined by VNA.

The resonance peaks of the quartz crystal are shifted and broadened by contact with the liquid sample. The spectra after the contact are approximated as follows

$$V'_n(\nu) = a'\nu + b' + \alpha\sum_k \frac{V_{n,k}}{1 + \dfrac{\nu - (\nu_{n,k} - \delta\nu_n)}{(\Delta\upsilon_n + \delta\Delta\upsilon_n)}\mathrm{i}} \tag{11}$$

Here, we assume that the shifts and the broadenings, denoted as $\delta\nu_n$ and $\delta\Delta\nu_n$, respectively, are common to all spurious modes and that the relative intensity of the spurious modes are not affected by the presence of the sample. The representative spectra are shown in Figures 1 and 2 together with fitting curves. The experimental data are reproduced well by eqs 9 and 11.

The complex shear viscosity is evaluated from $\delta\nu_n$ and $\delta\Delta\nu_n$ according to the equation as[6]

$$\eta(\nu_{n,0}) \equiv \eta'(\nu_{n,0}) - \mathrm{i}\eta''(\nu_{n,0}) = \frac{\pi Z_Q^2}{2\rho\nu_{n,0}{\nu_{0,0}}^2}[2\delta\nu_n\delta\Delta\nu_n - (\delta\Delta{\nu_n}^2 - \delta{\nu_n}^2)\mathrm{i}] \tag{12}$$

where Z_Q and ρ stand for the shear impedance of the quartz and the mass density of the sample solution, respectively. The values of the density are taken from the literature.[12–15] The measurements on a sample are performed twice, and their values are averaged after the scattered data are omitted. The criterion to discard data is that $\eta'(\nu)$ deviates from its adjacent values by more than 20% and that the deviation is not reproducible.

3.4. Validation of the Spectrometer. The quality of the resonator is characterized by the Q factor, whose definition is given by

$$Q \equiv \frac{\nu_{n,0}}{2\Delta\nu_n} \tag{13}$$

The Q factors in the absence of sample liquids are plotted in Figure 3.

The recommended value of the Q factor for shear relaxation spectroscopy is higher than 10^5.[6] The Q factor of our resonator exceeds the recommended value only between 35 and 105 MHz.[16]

Since our measurement of shear relaxation between 110 and 210 MHz using VNA is performed for the first time in this work, we shall show the test measurement on the aqueous solution of

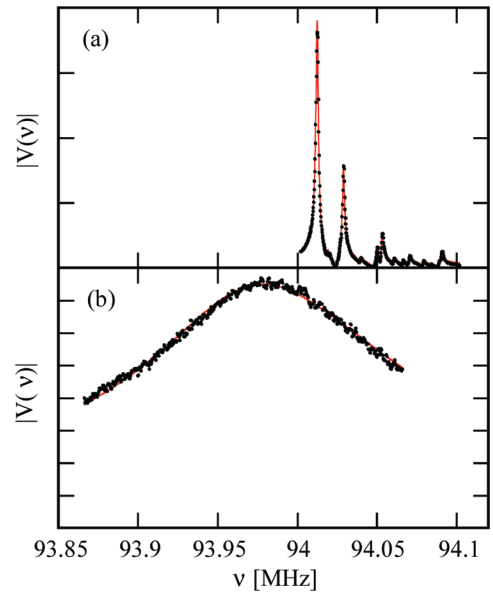

Figure 1. The 19th-order transmission spectra in the RF measurement before and after the contact with [bmim][PF_6] at 25 °C are plotted in panels (a) and (b), respectively. The experimental data and fitting curves are shown by black circles and red curves, respectively. In panel (b), the fitting curve is hardly visible because it is almost overlapped with the experimental data.

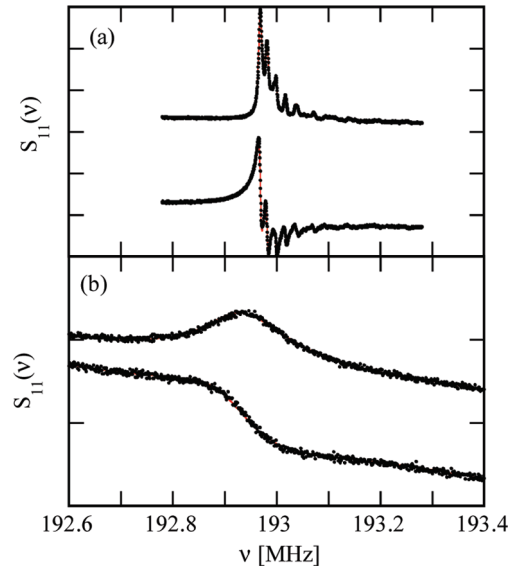

Figure 2. The 39th-order transmission spectra in the VNA measurement before and after the contact with [bmim][PF_6] at 25 °C are plotted in panels (a) and (b), respectively. The upper and lower curves in both panels represent the real and imaginary parts, respectively. The meanings of the symbols are the same as those in Figure 1.

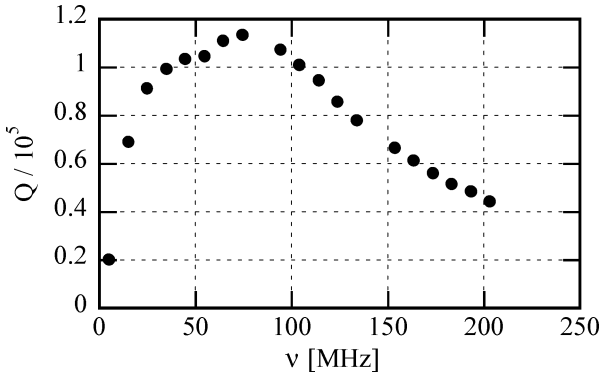

Figure 3. Q factors of the resonator without sample liquids are plotted as a function of the frequency.

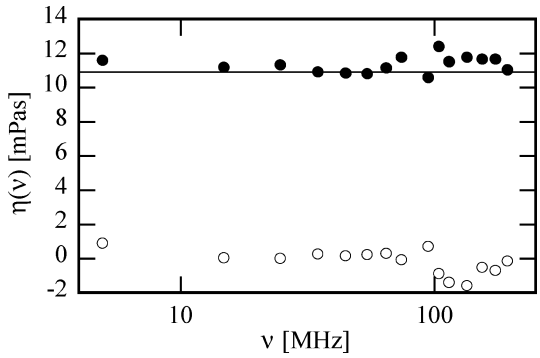

Figure 4. The frequency-dependent shear viscosity of the aqueous solution of glycerin at 20 °C and 60 wt % is shown as a function of the frequency. The real and imaginary parts are plotted as the filled and open circles, respectively. The zero-frequency value taken from the literature[17] is also demonstrated as the horizontal line for comparison.

glycerin. Glycerin (guaranteed grade, Wako) is mixed with distilled water without further purification. The measurements are performed at 20 °C, and the density used in the analysis is taken from the literature.[17]

Figure 4 shows a typical result at the concentration of 60 wt %. The real part of the shear viscosity is almost independent of the frequency, and its absolute value is close to that of the zero-frequency one reported in the literature.[17] The imaginary part is almost zero, as is expected when the response of the shear stress is instantaneous. Similar results are obtained at other concentrations below 90 wt %, and we consider that our spectrometer is applicable up to 205 MHz, although the Q values shown in Figure 3 are not sufficiently large. The experimental error is estimated to be $|\Delta\eta(\nu)/\eta(\nu)| < 0.1$ between 15 and 95 MHz, and $|\Delta\eta(\nu)/\eta(\nu)| < 0.2$ at other frequencies.

4. Results and Discussions

4.1. Effect of the Anion. Figure 5 exhibits the shear relaxation spectra of [bmim][PF_6] and [bmim][TFSA] at 25 °C. In both cases, a large relaxation is found in the measured frequency range, and the real parts appear to converge to their respective zero-frequency values at the lowest frequency (5 MHz).

Since the shear impedance method probes solely the sample liquids near the quartz crystal, one may consider that our experimental results are affected by the interfacial properties of ionic liquids. The penetration depth of the shear wave, d_p, is theoretically given by[6]

$$d_p = \sqrt{\frac{\eta}{\pi\rho\nu}} \tag{14}$$

Roughly speaking, the shear viscosity within d_p from the electrode is averaged in the shear impedance spectroscopy. If we substitute $\eta = 0.1$ Pa s, $\rho = 1400$ kg/m^3, and $\nu = 200$ MHz as typical values, the value of d_p is equal to 340 nm. On the other hand, Ueno and co-workers very recently reported the shear viscosity of [bmim][TFSA] between two silica plates.[18] They found that the effective viscosity is independent of the distance between two plates, D, when D is larger than 10 nm, and the effective viscosity increases rapidly with decreasing D at $D < 10$ nm. Their experiment suggests that the interface affects the shear viscosity of the ionic liquid within the range of 10 nm. Since the penetration depth is much larger than 10 nm, we consider that the properties of the bulk liquid are mainly probed in our experiment.

As is mentioned in section 1, Makino and co-workers determined the ultrasonic absorption coefficients of the same ionic liquids at three different frequencies between 10 and 100 MHz and found that the absorption coefficients are dependent on frequency.[5] Although the ultrasonic relaxation may be caused by volume relaxation processes that do not affect the shear viscosity, they argued that there must be a relaxation of the shear viscosity because the amplitude of the ultrasonic relaxation is too large to ascribe it wholly to the bulk viscosity. In this work, we actually observe the shear relaxation in the same frequency range, and our experimental results are direct proof of their prediction.

The dotted curves show the Debye relaxation function, eq 6, to reproduce $\eta(\nu)$ of [bmim][PF_6]. The relaxation time, $\tau = 1.1$ ns, is determined in order to match the frequency where $\eta'(\nu) = \eta(0)/2$. In contrast to the ultrasonic relaxation performed by Makino and co-workers,[5] our experimental results are not reproduced by a Debye function. It means that more than one relaxation time, or preferably the distribution of the relaxation times, is required in order to describe our experimental results by the superposition of the Debye functions. The viscosity of ionic liquids usually shows non-Arrhenius temperature dependence and is often described by the Vogel−Fulcher−Tammann equation,[12,14,15] which is in harmony with the presence of the relaxation time distribution revealed in this work.

The presence of the shear relaxation is also predicted by many molecular dynamics (MD) simulation studies.[19–22] In the MD

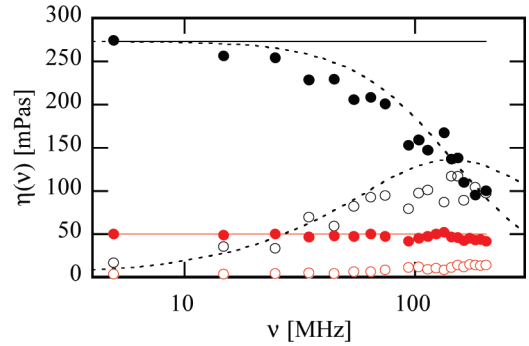

Figure 5. The frequency-dependent shear viscosities of [bmim][PF_6] (black) and [bmim][TFSA] (red) at 25 °C are shown as functions of the frequency. The real and imaginary parts are plotted as the filled and open circles, respectively. The zero-frequency values taken from the literatures[12,13] are also exhibited as the horizontal solid lines for comparison. The dotted curves are the real and imaginary parts of the Debye function, eq 6, whose relaxation time is $\tau = 1.1$ ns.

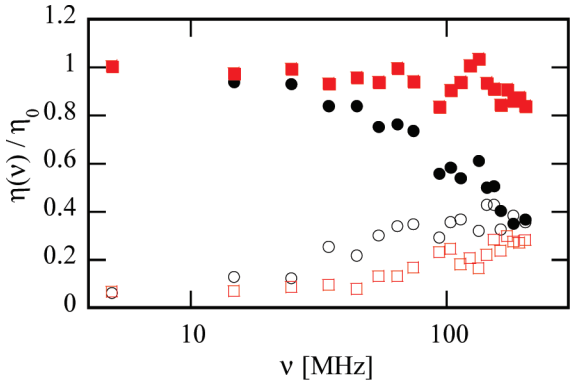

Figure 6. The normalized shear relaxation spectra of [bmim][PF_6] (red squares) and [bmim][TFSA] (black circles) are plotted against the frequency. The real and imaginary parts are shown as the filled and open symbols, respectively.

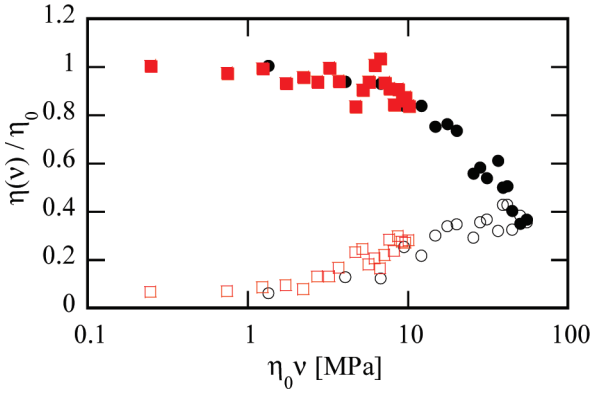

Figure 7. The normalized shear relaxation spectra of [bmim][PF_6] and [bmim][TFSA] are plotted against the product of the frequency and zero-frequency shear viscosity. The meanings of the symbols are the same as those of Figure 6.

simulations, the shear viscosity is calculated from the time correlation functions of the shear stress through the Kubo−Green formula, eq 1. It often takes several hundred picoseconds in order to achieve the convergence of the time integral of the right-hand side of eq 1, which corresponds to the presence of the shear relaxation at several hundred MHz.

According to the large amplitude of the shear relaxation shown in Figure 5, we can consider that the zero-frequency shear viscosity is determined by the observed relaxation process. Therefore, the analysis of this relaxation can provide us the information on the microscopic origin of the shear viscosity, that is, the reason why [bmim][PF_6] is more viscous than [bmim][TFSA].

In Figure 6, the normalized shear relaxation spectra are plotted against ν. According to the discussions in section 2, the normalized spectra reduce to a single master curve as the function of frequency when the relaxation amplitude (shear modulus) is the principal cause of the difference in viscosity. As shown in Figure 6, however, the relaxation frequency of [bmim][PF_6] is lower than that of [bmim][TFSA], and the normalized spectra do not agree with each other. Therefore, the relaxation amplitude alone cannot explain the lower viscosity of [bmim][TFSA] than that of [bmim][PF_6].

Figure 7 exhibits the normalized spectra as a function of $\eta_0\nu$. Both spectra lie on a single curve on this scale, which indicates that the relaxation times of these two liquids are different with little change in the relaxation amplitude, A, and that the functional form of $\tilde{\phi}_0(\nu)$ is also conserved within the frequency range of our measurement. In other words, the viscosity of

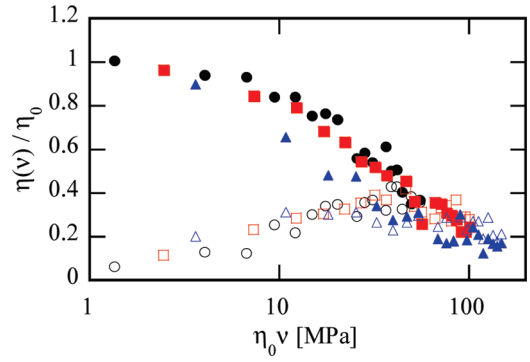

Figure 8. The normalized shear relaxation spectra of [bmim][PF_6] (black circles), [hmim][PF_6] (red squares), and [omim][PF_6] (blue triangles) at 25 °C are plotted against the product of the frequency and zero-frequency shear viscosity. The filled and open symbols denote the real and imaginary parts, respectively.

[bmim][TFSA] is smaller than that of [bmim][PF_6] because the relaxation time of the former is smaller than that of the latter.

4.2. Effect of the Cation. Figure 8 shows the normalized shear relaxation spectra of three different PF_6^- salts, [bmim][PF_6], [hmim][PF_6], and [omim][PF_6] at 25 °C as the functions of $\eta_0\nu$. Contrary to Figure 7, the three spectra do not fall onto a single curve on this horizontal axis. The reduced relaxation frequency decreases with increasing the length of the alkyl chain of the cation, which means that the increase in the relaxation time is larger than that of zero-frequency shear viscosity. Since the zero-frequency shear viscosity is related to the product of the relaxation time and the relaxation amplitude, the latter must decrease with lengthening of the alkyl chain of the cation. In addition, the distribution of the relaxation time appears to become broader with increasing chain length. The broader distribution of the relaxation time indicates the more stretched relaxation of the time correlation function, $\phi(t)$ in eq 1.

Recent studies on ionic liquids have revealed that the structure of the ionic liquid is heterogeneous, composed of polar and nonpolar domains. The presence of the heterogeneous structure was first suggested by a molecular dynamics (MD) simulation[23] and proven by X-ray diffraction experiments.[24] The intermolecular interaction within the polar domain is strong due to the electrostatic interactions between ions. On the other hand, the intermolecular interaction in the nonpolar domain is expected to be small, and some experiments show that a solute in the nonpolar solute feels a friction force as small as that within liquid alkanes.[25,26] The heterogeneity of the structure increases with increasing length of the alkyl chain.[23,24] In addition to the heterogeneity associated with the domain structure, the imidazolium cation possesses various conformations of its alkyl chain,[27] which can be a source of other heterogeneity.

On the basis of the idea of a heterogeneous structure, our experimental results in Figure 8 can be realized as follows. First, the lengthening of the alkyl chain leads to the increase in the volume of the nonpolar domain, which decreases the mean intermolecular interaction per unit volume, leading to the decrease in the relaxation amplitude which corresponds to the high-frequency shear modulus. Second, if the relaxation is associated with the heterogeneous structure, its development will result in the retardation of its relaxation time. Third, the heterogeneity of the liquid structure can be a reason for the wide distribution of the relaxation time.

Although the discussion above relates the relaxation time distribution with the static heterogeneity, there is another source

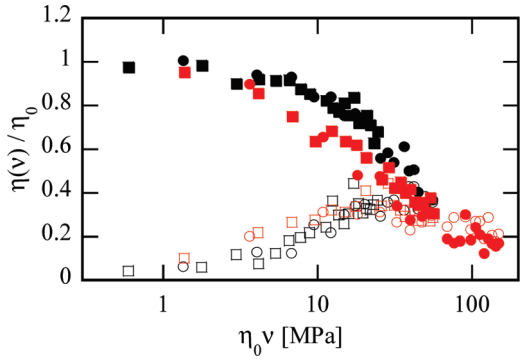

Figure 9. The normalized shear relaxation spectra of [bmim][PF_6] (black) and [omim][PF_6] (red) at 25 (squares) and 40 °C (circles) are plotted against the product of the frequency and zero-frequency shear viscosity. The filled and open symbols denote the real and imaginary parts, respectively.

of the distribution of the relaxation time. Recent studies show that the dynamics of supercooled liquids is characterized by dynamic heterogeneity.[28] Even though the static structure of the supercooled liquid is homogeneous, it is momentarily composed of mobile and less mobile regions. The dynamic heterogeneity develops as the liquid is supercooled deeper. Since [omim][PF_6] is more viscous than [bmim][PF_6], the slow dynamics of the former is regarded as more developed than that of the latter, which can be a reason for the wider distribution of the relaxation time of the former. If it were really the case, the difference in the relaxation time distribution could be understood in terms of the dynamics of a supercooled liquid in general, without resorting to the heterogeneous structure peculiar to ionic liquids.

Figure 9 shows the shear relaxation spectra of [bmim][PF_6] and [omim][PF_6] at two different temperatures, 25 and 40 °C. The spectra of the same sample at different temperatures overlap with each other well on the $\eta_0\nu$ scale. The temperature dependence of the shear viscosity is thus attributed to that of the relaxation time, that is, the decrease in viscosity with increasing temperature is due to the reduction of the relaxation time. On the other hand, the difference in the spectra of [bmim][PF_6] and [omim][PF_6] remains the same at the elevated temperature. In particular, since the shear viscosity of [bmim][PF_6] at 25 °C (273 mPa s) is similar to that of [omim][PF_6] at 40 °C (277 mPa s), their degrees of development of the slow dynamics can be regarded as equal. We could hence expect that their distribution widths of the relaxation time would also be similar if the dynamic heterogeneity were the reason for the difference in the distribution width. Therefore, we consider that the broader distribution of the relaxation time of [omim][PF_6] is better ascribed to its static liquid structure.

4.3. Comparison with Electrical Conductivity. Electrical conductivity is another transport property of ionic liquids that has been studied intensively because it is of practical importance when ionic liquids are used as the electrolytes of electrochemical devices.

The direct-current (DC) electrical conductivity, σ_0, is related to the zero-frequency shear viscosity, η_0, empirically by the Walden rule, which states that σ_0 is inversely proportional to η_0. As for ionic liquids, the Walden rule has been tested with respect to the temperature dependence and various combinations of ions.[2,29]

The Walden rule can be derived theoretically from the Stokes−Einstein and Nernst−Einstein relationships. The former states that the frictional force on a ion is given by the hydrodynamic Stokes law, where the surrounding medium around the ion is regarded as the viscous continuum. The latter is the approximation that the diffusive motions of the ions contributing to the electric current are uncorrelated. Since both approximations are not expected to hold in ionic liquids where ions are closely packed, we need to seek another microscopic basis for the validity of the Walden rule in the case of ionic liquids.

In this section, we extend the Walden rule to the frequency-dependent one in order to clarify its microscopic origins. A similar approach has already been performed by Šantić and co-workers on an ionic liquid supercooled down to 200 K,[3] and the shear impedance spectroscopy employed in this work has enabled us to perform experiments at room temperature.

Suppose that the inverse proportionality between σ_0 and η_0 is extended to the corresponding frequency-dependent transport coefficients, $\sigma(\nu)$ and $\eta(\nu)$. The normalized relaxation spectra are then related to each other as

$$\frac{\eta(\nu)}{\eta_0} = \frac{\sigma_0}{\sigma(\nu)} \tag{15}$$

Since the frequency dispersion of these spectra are closely related to the microscopic mechanism of the transport coefficients, we can compare the microscopic processes involved in the shear viscosity and electrical conductivity by the comparison of right- and left-hand sides of eq 15.

The frequency-dependent electrical conductivity is evaluated from the dielectric relaxation spectrum. The dielectric relaxation spectrum reported in the literature, $\Delta\varepsilon(\nu)$, is calculated from the total electric susceptibility determined in experiments directly, $\varepsilon(\nu)$, as[30]

$$\Delta\varepsilon^*(\nu) = \varepsilon^*(\nu) - \frac{\sigma_0}{2\pi i\nu} \tag{16}$$

and often analyzed under the assumption that $\Delta\varepsilon(\nu)$ is mainly ascribed to the reorientational modes of ions. The $\varepsilon^*(\nu)$ of conductive liquids behaves as $\sigma_0/2\pi i\nu$ in the low-frequency limit, and the singularity at $\nu = 0$ is removed by the second term of the right-hand side. On the other hand, $\sigma(\nu)$ is related to $\varepsilon(\nu)$ as

$$\sigma(\nu) = 2\pi i\nu\varepsilon(\nu) \tag{17}$$

We can convert $\Delta\varepsilon(\nu)$ into $\sigma(\nu)$ with the combination of eqs 16 and 17.

Figure 10 shows the inverse of the frequency-dependent normalized electrical conductivity of [bmim][PF_6] at 25 °C. The shear relaxation spectrum is plotted for comparison. The relaxation frequency of the reciprocal electrical conductivity is about twice as large as that of the shear viscosity. The higher relaxation frequency of the conductivity was reported by Šantić and co-workers at about 200 K,[3] and our result is in harmony with theirs. The difference between the dielectric and acoustic relaxation times was also reported by Fukuda and co-workers.[4] The deviation of the relaxation time of the electric modulus from other relaxation times such as solvation dynamics and reorientational and thermal relaxations was also reported by Richert and co-workers.[31,32] We recently performed a theoretical calculation on a model ionic liquid, dimethylimidazolium chloride, based on the mode-coupling theory and found that the relaxation of the ionic conductivity is faster than that of shear viscosity, as is observed in this work.[33] The conductivity

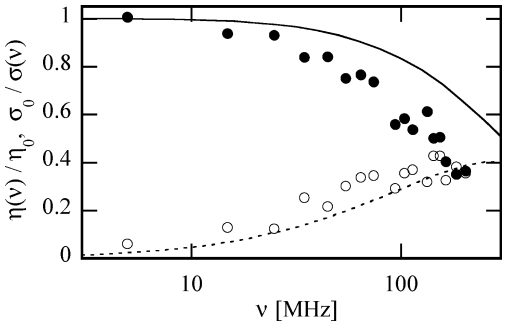

Figure 10. The normalized shear relaxation spectrum, $\eta(\nu)/\eta_0$, of [bmim][PF_6] at 25 °C is compared with the normalized reciprocal conductivity dispersion spectrum, $\sigma_0/\sigma(\nu)$, which is calculated from the dielectric relaxation spectrum in the literature.[34] The real and imaginary parts of $\eta(\nu)/\eta_0$ are plotted as the filled and open circles, respectively, while those of $\sigma_0/\sigma(\nu)$ are drawn by the solid and dotted curves, respectively.

dispersion spectrum is evaluated from the dielectric relaxation spectrum reported by Nakamura and Shikata.[34] Although their spectrum is slightly different from that of Hunger and coworkers,[35] the difference is far smaller than that between $\eta(\nu)/\eta_0$ and $\sigma_0/\sigma(\nu)$. Since the decoupling between the shear viscosity and electrical conductivity exists on the frequency axis, we need further consideration of mechanisms of the relationship between their zero-frequency values.

One may consider that the decoupling between the viscosity and conductivity is not surprising because the former is related to both the polar and nonpolar domains while the latter is predominantly related to the former. However, the relaxation of the latter would be slower if it were really the case because the polar domain is more viscous than the nonpolar one.

It is to be noted that the comparison above depends on the assignment of the relaxation of the electrical conductivity shown in Figure 10. In the analysis of the dielectric relaxation spectra, the translational motion of ions is usually assumed Markovian, and the apparent dispersion of the electrical conductivity is wholly ascribed to the reorientational relaxation of the cation.[34,35] Although we recently showed by mode-coupling theoretical calculations that the conductivity dispersion in the 100 MHz region mainly originates from the translational mode in the case of liquid dimethylimidazolium chloride,[33] the reorientational mode also makes a non-negligible contribution. What we want to compare are the shear viscosity and translational mobility of ions. The difference between them would be larger if we subtracted the contribution of the reorientational modes from $\sigma(\nu)$.

The Walden rule is based on the Stokes−Einstein and Nernst−Einstein relationships. The decoupling between the shear viscosity and electrical conductivity can thus be caused by either the decoupling between the shear viscosity and diffusivity or that between the diffusivity and electrical conductivity. The decoupling between the molecular mobility and shear viscosity has been reported on various supercooled liquids, and it is usually explained by the dynamic heterogeneity.[36,37] On the other hand, our theoretical calculation shows that the electrical conductivity can be decoupled from the self-diffusivity even if the latter is coupled to the shear viscosity.[33] In order to clarify which is the reason for the decoupling between the shear viscosity and electrical conductivity revealed in this work, we need to measure the spectra of self-diffusivities of ions in experimental ways such as an inelastic neutron scattering measurement.

5. Summary

The frequency-dependent shear viscosities of four representative imidazolium-based ionic liquids are determined at 5−205 MHz with shear impedance spectroscopy. We have succeeded in observing the shear relaxation of ionic liquids at ambient conditions experimentally for the first time, to our best knowledge.

The mechanisms of the variation of zero-frequency shear viscosities are discussed based on the shear relaxation spectra. As for the temperature dependence, the decrease in the relaxation time explains the decrease in the shear viscosity with increasing temperature. The difference between the shear viscosities of [bmim][PF_6] and [bmim][TFSA] is also ascribed to the difference in the relaxation time. On the other hand, when the alkyl chain of the cation is lengthened, the shear viscosity increases because the increase in the relaxation time overwhelms the decrease in the shear modulus. In addition, the broadening of the relaxation time distribution is also observed.

The difference in the relaxation spectra with cations of various lengths of alkyl chains is discussed in terms of the heterogeneity of the liquid structure. Some recent studies on ionic liquids have shown that the structure of the ionic liquids is heterogeneous, composed of polar and nonpolar domains. The strong Coulombic interaction works in the polar domain, whereas the microscopic viscosity of the nonpolar domain is as low as that of liquid alkanes. The heterogeneity develops with increasing the length of the alkyl chain. The larger heterogeneity of the equilibrium structure can lead to the heterogeneity of the relaxation time. The larger-scale structure requires longer time to relax, which explains the increase in the relaxation time with lengthening of the alkyl chain. Since the intermolecular interaction between ions is weak in the nonpolar domain, the increase in its volume can decrease the amount of intermolecular interaction per volume, which explains the decrease in the shear modulus. However, the clarification of the microscopic origin of the relaxation is necessary for detailed discussions, for which further theoretical, computational, and experimental studies will be required.

The shear relaxation spectrum of [bmim][PF_6] is compared with the frequency-dependent electrical conductivity. The relaxation frequency of the latter is about twice larger than that of the former, which indicates partial decoupling between the shear viscosity and ionic current. The decoupling is in harmony with a previous experiment under supercooled conditions and our theoretical study based on the mode-coupling theory. We consider that the comparison between shear relaxation and conductivity dispersion spectra at various thermodynamic conditions on many ionic liquids gives valuable information to understand the relationship between the zero-frequency shear viscosity and DC electrical conductivity.

The presence of the shear relaxation also possesses some implications for chemical reactions in ionic liquids.[38–41] The rates of unimolecular chemical reactions have often been related to the shear viscosity of solvents when the reaction involves a change in atomic geometries, as is the case of isomerization reactions and nonradiative relaxations. The theoretical basis of the relationship was given by Grote and Hynes,[42] who related the reaction rate to the friction coefficient along the reaction coordinate at the transition state. The friction coefficient is dependent on frequency in general, and the frequency effective to the reaction is determined by the curvature of the potential energy surface at the transition state. Apart from the long-standing question on the use of macroscopic shear viscosity for the microscopic friction coefficient, the replacement of the zero-

frequency viscosity for the high-frequency one is not justified when the shear viscosity is dependent on frequency. Some viscosity-dependent reactions occur on the time scale of picoseconds, whereas the relaxation times of the shear viscosity are from several hundred of picoseconds to several nanoseconds in this work. Since ionic liquids behaves elastically on the time scale of picoseconds, fast reactions in ionic liquids may have to be regarded as those occurring in amorphous solids.

Acknowledgment. This work is supported by Research Grants from the Mitsubishi Chemical Corporation Fund.

References and Notes

(1) Ueno, K.; Tokuda, H.; Watanabe, M. *Phys. Chem. Chem. Phys.* **2010**, *12*, 1649.
(2) Umecky, T.; Saito, Y.; Tsuzuki, S.; Matsumoto, H. *ECS Trans.* **2009**, *16*, 39.
(3) Šantić, A.; Wrobel, W.; Mutke, M.; Banhatti, R. D.; Funke, K. *Phys. Chem. Chem. Phys.* **2009**, *11*, 5930.
(4) Fukuda, M.; Terazima, M.; Kimura, Y. *J. Chem. Phys.* **2008**, *128*, 114508.
(5) Makino, W.; Kishikawa, R.; Mizoshiri, M.; Takeda, S.; Yao, M. *J. Chem. Phys.* **2008**, *129*, 104510.
(6) Behrends, R.; Kaatze, U. *Meas. Sci. Technol.* **2001**, *12*, 519.
(7) Behrends, R.; Kaatze, U. *J. Phys. Chem. A* **2000**, *104*, 3269.
(8) Behrends, R.; Kaatze, U. *J. Phys. Chem. A* **2001**, *105*, 5829.
(9) Yamaguchi, T.; Hayakawa, M.; Matsuoka, T.; Koda, S. *J. Phys. Chem. B* **2009**, *113*, 11988.
(10) McHale, G.; Hardacre, C.; Ge, R.; Doy, N.; Allen, R. W. K.; MacInnes, J. M.; Bown, M. R.; Newton, M. I. *Anal. Chem.* **2008**, *80*, 5806.
(11) Boon, J. P.; Yip, S. *Molecular Hydrodynamics*; McGraw-Hill, New York, 1980.
(12) Tokuda, H.; Ishii, K.; Susan, M. A. B. H.; Tsuzuki, S.; Hayamizu, K.; Watanabe, M. *J. Phys. Chem. B* **2006**, *110*, 2833.
(13) Fan, W.; Zhou, Q.; Sun, J.; Zhang, S. *J. Chem. Eng. Data* **2009**, *54*, 2307.
(14) Tomida, D.; Kumagai, A.; Kenmochi, S.; Qiao, K.; Yokoyama, C. *J. Chem. Eng. Data* **2007**, *52*, 577.
(15) Harris, K. R.; Kanakubo, M.; Woolf, L. A. *J. Chem. Eng. Data* **2006**, *51*, 1161.
(16) The Q values shown in our previous work (ref 9) were wrongly defined to be twice larger than the correct one, eq 13.
(17) *The Japan Society of Mechanical Engineering, JSME data book: thermophysical properties of fluids*; The Japan Society of Mechanical Engineering: Tokyo, 1983.
(18) Ueno, K.; Kasuya, M.; Watanabe, M.; Mizukami, M.; Kurihara, K. *Phys. Chem. Chem. Phys.* **2010**, *12*, 4066.
(19) Bhargave, B. L.; Balasubramanian, S. *J. Chem. Phys.* **2005**, *123*, 144505.
(20) Castro, C. R.; Vega, L. F. *J. Phys. Chem. B* **2006**, *110*, 14426.
(21) Schröder, C.; Wakai, C.; Weingärtner, H.; Steinhauser, O. *J. Chem. Phys.* **2007**, *126*, 084511.
(22) Van-Oanh, N.-T.; Houriez, C.; Rousseau, B. *Phys. Chem. Chem. Phys.* **2010**, *12*, 930.
(23) Lopes, J. N. A. C.; Pádua, A. A. H. *J. Phys. Chem. B* **2006**, *110*, 3330.
(24) Triolo, A.; Russina, O.; Bleif, H.-J.; Cola, E. D. *J. Phys. Chem. B* **2007**, *111*, 4641.
(25) Xiao, D.; Hines. Jr., L. G.; Bartsch, R. A.; Quitevis, E. L. *J. Phys. Chem. B* **2009**, *113*, 4544.
(26) Fruchey, K.; Fayer, M. D. *J. Phys. Chem. B* **2010**, *114*, 2840.
(27) Endo, T.; Kato, T.; Tozaki, K.; Nishikawa, K. *J. Phys. Chem. B* **2010**, *114*, 407.
(28) Yamamoto, R.; Onuki, A. *Phys. Rev. E* **1998**, *58*, 3515.
(29) Xu, W.; Cooper, E. I.; Angell, C. A. *J. Phys. Chem. B* **2003**, *107*, 6170.
(30) The definition of $\varepsilon(\nu)$ varies among the literature. For example, Buchner's group at Regensburg defines $\varepsilon(\nu)$ as the spectra after the subtraction of the contribution of DC conductivity,[35] so that $\varepsilon(\nu)$ in their papers corresponds to $\Delta\varepsilon(\nu)$ in this work. We follow the definition by Shikata and Nakamura because the spectrum shown in Figure 10 is taken from their paper.[34]
(31) Ito, N.; Richert, R. *J. Phys. Chem. B* **2007**, *111*, 5016.
(32) Huang, W.; Richert, R. *J. Chem. Phys.* **2009**, *131*, 184501.
(33) Yamaguchi, T.; Koda, S. *J. Chem. Phys.* **2010**, *132*, 114502.
(34) Nakamura, K.; Shikata, T. *ChemPhysChem* **2010**, *11*, 285.
(35) Hunger, J.; Stoppa, A.; Schrödle, S.; Hefter, G.; Buchner, R. *ChemPhysChem* **2009**, *10*, 723.
(36) Voronel, A.; Veliyulin, E.; Machavariani, V. S.; Kisliuk, A.; Quitmann, D. *Phys. Rev. Lett.* **1998**, *80*, 2630.
(37) Xia, X.; Wolynes, P. W. *J. Phys. Chem. B* **2001**, *105*, 6570.
(38) Ozawa, R.; Hamaguchi, H. *Chem. Lett.* **2001**, *30*, 736.
(39) Fukuda, M.; Kajimoto, O.; Terazima, M.; Kimura, Y. *J. Mol. Liq.* **2007**, *134*, 49.
(40) Mali, K. S.; Dutt, G. B.; Mukherjee, T. *J. Chem. Phys.* **2008**, *128*, 124515.
(41) Khurmi, C.; Berg, M. *J. Phys. Chem. Lett.* **2010**, *1*, 163.
(42) Grote, R. F.; Hynes, J. T. *J. Chem. Phys.* **1980**, *73*, 2715.

JP1024137